




Exchange interaction for Mn acceptors in GaAs: Revealing its strong deformation dependenceI. V. Krainov ^{1,*}, K. A. Baryshnikov ^{1,†}, A. A. Karpova ^{1,2} and N. S. Averkiev¹¹*Ioffe Institute, 194021 St. Petersburg, Russia*²*Saint Petersburg Electrotechnical University, 197022 St. Petersburg, Russia*

(Received 17 January 2023; revised 30 March 2023; accepted 12 April 2023; published 2 May 2023)

In this paper we calculate the exchange interaction constant between the manganese ion inner electronic d -shell and GaAs valence band bound hole using their microscopic multiparticle wave functions. We reveal its parametric dependence on crystal lattice deformations and find that it could be about and even more than dozens of a percent when the strain tensor reaches values of 10^{-3} – 10^{-2} . This fact is in accordance with the previous hypothesis of deformation dependence of Mn acceptors in a GaAs fine energy structure obtained from Raman spectroscopy; we show that this dependence has the same magnitude. Also, we resolve here the problem of a substantial high-temperature mismatch between well-developed theory and experimental data for the static magnetic susceptibility of Mn ions in GaAs. We show by numerical estimates and calculations that quite a strong parametric dependence of the exchange coupling value on GaAs lattice expansion determines the high-temperature (above 50 K) magnetic susceptibility reduction as well.

DOI: [10.1103/PhysRevB.107.174401](https://doi.org/10.1103/PhysRevB.107.174401)**I. INTRODUCTION**

Modern material science is focused on functional materials combining different properties with maximal functionality. Some of these important kinds of materials are magnetic semiconductors mixing electrical, optical, and magnetic properties. Different ways to control these properties merge into important directions of research, including the production of new compounds [1–6], nanostructure design [1,7–11], and the investigation of the effects of external forces application [12–16]. One of the most well-known functional materials is GaMnAs [17–20]. In this material, manganese ion with its inner magnetic $3d$ -shell containing five electrons brings magnetism to the GaAs semiconductor host. This is due to the exchange interactions between manganese's inner d -electrons with GaAs holes. Also, the manganese impurity acts as an acceptor increasing the hole concentration in the GaAs semiconductor crystal. For an isolated impurity the exchange interaction between the Mn half-filled d -shell with the total spin of electrons $5/2$ and localized hole in the Γ_8 symmetry state acting like a $3/2$ spin results in an initially 24-fold degenerate state split into four sublevels with total angular momentum $F = 1, 2, 3, 4$ with $F = 1$ being the ground state [16]. Here we focus our attention on this exchange interaction between the isolated manganese ion and a hole localized on it.

The exchange interaction constant A for the Mn acceptor consists of two parts. The first part includes the exchange between Mn d -shell orbital electrons and the Bloch orbital

of the Γ_8 hole. The second part includes the value of the hole envelope at the impurity site, i.e., the probability to couple with the half-filled d -shell as a whole. In all previous works [21–23] in which such an interaction was discussed, only the second part (the value of the hole envelope at the impurity site) was assumed to change in different conditions, while the first part (the exchange between Bloch functions) was assumed to be unperturbed and its value was postulated [16]. The deformation influence on the envelope part of the exchange constant was investigated in Ref. [23], but it was found that it changes by less than one percent at pressures on the limit of GaAs hardness. The purpose of this work is to calculate the exchange interaction value between Bloch functions of the Mn d -shell and the Γ_8 hole bound from the GaAs valence band, and to treat its dependence on deformation. We demonstrate that this part of the exchange interaction is sensitive to the presence of crystal strains.

Previously, the assumption of a strong dependence of exchange constant A on the crystal deformation played a crucial role in the study of the fine-structure of an isolated Mn acceptor in GaAs. This was investigated using Raman spin-flip scattering and its dependence on magnetic fields and external deformations at helium temperatures [24]. The theoretical fit of intra- and inter-transitions between Mn-hole levels based on a standard model of the Mn acceptor eigenstates was also carried out in Ref. [24], but to make a satisfactory agreement between all experimental curves and theoretical calculations the deformation dependence of the exchange interaction constant was phenomenologically proposed and its value was estimated from comparison with the experiment. The exchange interaction value changes by 20% for the pressure 5 kbar, which is about half of the GaAs critical value of hardness, and hence this change is much larger than previously mentioned—nearly one percent dependence on the hole envelope wave-function change.

*igor.krainov@mail.ru

†barysh.1989@gmail.com

Independently, there were taken drastically different measurements of static magnetic susceptibility behavior in a wide temperature range in GaAs samples with a low concentration of Mn ions. The first experiments were made by Andrianov's group [25], but their work contained an irrelevant theoretical model of the Mn center, which mismatched with several low-temperature properties of the center. Other measurements were carried out by Frey's group and reported in Ref. [26], where the relevant theoretical model was applied, which, however, has some discrepancies with the data at the very high temperature edge. The findings of these studies are that the theoretical fit based on that true and now standard Mn-hole interaction model of experimental data is in good agreement with the low-temperature region below 50 K. However, for the high-temperature region, there is a reduction of magnetic susceptibility compared with the theoretical prediction, which is still puzzling. A recent paper [16] containing a deep review of different experimental and theoretical facts about the Mn center in GaAs proposed a hypothesis that the variance mentioned above could be explained by the Jahn-Teller effect (JTE).

In this paper we also test this hypothesis (see the Supplementary Material [27] and also Refs. [16,25,28–32] and references therein). It is known from many other experimental facts [16] that the Mn ground $F = 1$ state is unaffected by the static Jahn-Teller distortion, so only dynamical JTE should be tested [32]. Moreover, one can show that at high temperatures, there is only one way for dynamical JTE to occur, which is reduced to the Jahn-Teller interaction of a hole in the Γ_8 state with local lattice distortions. As we show (see Ref. [27], Part 2), the high temperature dependence of magnetic susceptibility is negligibly dependent on the Jahn-Teller effect and ceases quite rapidly as temperature increases, which cannot explain the observed reduction of the magnetic susceptibility discussed above. Also we test a hypothesis of the crystal field influence, but this also cannot explain the magnetic susceptibility reduction at high temperatures (see Ref. [27], Part 1). Here we show that if we link the phenomenological dependence of the exchange interaction value on the external deformation from Ref. [24] with the thermal expansion coefficient of the crystal, the problem of high-temperature magnetic susceptibility reduction can be elegantly resolved.

In this paper we will calculate the Mn-hole exchange-interaction value part associated with the Bloch wave functions overlap. Then we provide an estimate for this strain dependence. Note that the trace of the strain tensor for the pressure about 5 kbar is in the range of 10^{-3} – 10^{-2} , and it is quite surprising how it can lead to a strong dependence of the exchange constant of $\sim 20\%$. We elaborate and explain a simple mechanism that could explain this fact. Further, we show that such purely theoretical estimates result in a similar variation for the Mn-hole exchange constant on stress that was assumed in Ref. [24], which has the same order of value. Finally, we show by direct calculations that the obtained dependence of A on the crystal strains ε , which theoretically fit the Mn fine-energy structure [24], leads to a better agreement

between high-temperature magnetic-susceptibility calculation results and the experimental data. We also believe that the developed model could be applied to other magnetic impurities and hosts with appropriate modifications in symmetry analysis.

II. THEORY

A. Exchange Hamiltonian and representation of total angular momenta $F = 1, 2, 3$, and 4

The eigenstates of the Mn acceptor are composed of the sixfold degenerate states of Mn ion d -shell electrons in the ground state with a total spin $S = 5/2$ and the fourfold degenerate state of a localized hole having the Γ_8 symmetry, which corresponds to the total angular momentum $J = 3/2$. Further, to simplify all conclusions, we will work in the hole basis of the d -shell, which has the same properties as the electronic one, because the shell is half-filled and one-particle states simply have opposite spins. These eigenstates are split by the exchange interaction between the half-filled d -shell and the localized hole resulting in the total angular momentum states $F = 1, 2, 3, 4$ with a corresponding degeneracy equal to $2F + 1$.

So if we assume that the exchange interaction between the ion's d -shell and the hole is described by only one constant A , i.e., if we set the corresponding Hamiltonian as

$$\hat{H}_{\text{ex}} = A(\hat{S} \cdot \hat{J}) = \frac{A}{2}(\hat{F}^2 - \hat{S}^2 - \hat{J}^2),$$

$$\hat{F} = \hat{S} + \hat{J}, \quad (1)$$

then we can easily find out all its energy eigenvalues, which are $A[F(F + 1) - S(S + 1) - J(J + 1)]/2$. All other possible terms proportional to $(\hat{S} \cdot \hat{J})^2$ and $(\hat{S} \cdot \hat{J})^3$ are connected to the second-order and higher-order perturbation terms of the Coloumb interaction causing a change of the spin projections of the d -shell electrons. We will neglect such terms because the energy of the spin-spin interaction between the d -shell electrons is assumed to be the largest among all other energies. This assumption allows us to consider all processes as if no changes in spin states of the inner shell electrons occur. Note also that there are no spin-orbit splittings in the d -shell, which is confirmed by the Raman scattering data of Mn^0 centers in GaAs, which has a g -factor strictly equal to 2 [24,33]. If there were four or six electrons in the d -shell of the ion, the nonzero orbital momentum appears and leads to additional orbitally dependent terms in the Hamiltonian [34]. However, as soon as we consider the half-filled shell, such effects become out of the scope of this paper.

To calculate the eigenenergies of \hat{H}_{ex} , it is sufficient to use the subset from the whole basis of acceptor states because of the spherical symmetry of the Hamiltonian. Let us consider such a subset consisting of only four wave functions $|F, F_z = 0\rangle$ (where $F = 1, 2, 3, 4$), and taking it from Ref. [16] (note that the prefactor coefficient in the $|2, 0\rangle$ function is changed to normalize correctly the wave function) one can write it

down as

$$|1, 0\rangle = \frac{1}{\sqrt{5}} \left\{ \Psi_{3/2}^S \Psi_{-3/2}^J - \Psi_{-3/2}^S \Psi_{3/2}^J \right. \\ \left. - \sqrt{\frac{3}{2}} \Psi_{1/2}^S \Psi_{-1/2}^J + \sqrt{\frac{3}{2}} \Psi_{-1/2}^S \Psi_{1/2}^J \right\}, \quad (2)$$

$$|2, 0\rangle = \sqrt{\frac{3}{7}} \left\{ \Psi_{3/2}^S \Psi_{-3/2}^J + \Psi_{-3/2}^S \Psi_{3/2}^J \right. \\ \left. - \sqrt{\frac{1}{6}} \Psi_{1/2}^S \Psi_{-1/2}^J - \sqrt{\frac{1}{6}} \Psi_{-1/2}^S \Psi_{1/2}^J \right\}, \quad (3)$$

$$|3, 0\rangle = \frac{1}{\sqrt{5}} \left\{ \sqrt{\frac{3}{2}} \Psi_{3/2}^S \Psi_{-3/2}^J - \sqrt{\frac{3}{2}} \Psi_{-3/2}^S \Psi_{3/2}^J \right. \\ \left. + \Psi_{1/2}^S \Psi_{-1/2}^J - \Psi_{-1/2}^S \Psi_{1/2}^J \right\}, \quad (4)$$

$$|4, 0\rangle = \sqrt{\frac{3}{7}} \left\{ \sqrt{\frac{1}{6}} \Psi_{3/2}^S \Psi_{-3/2}^J + \sqrt{\frac{1}{6}} \Psi_{-3/2}^S \Psi_{3/2}^J \right. \\ \left. + \Psi_{1/2}^S \Psi_{-1/2}^J + \Psi_{-1/2}^S \Psi_{1/2}^J \right\}. \quad (5)$$

Then one can calculate all the energy differences between \hat{H}_{exch} eigenstates as

$$E_{F+1} - E_F = \langle F+1, 0 | \hat{H}_{\text{exch}} | F+1, 0 \rangle - \langle F, 0 | \hat{H}_{\text{exch}} | F, 0 \rangle \\ = 2A, 3A, 4A. \quad (6)$$

This result could be obtained by taking a subset of four wave functions, which contain only zero projections of the total momentum on the z axis $\{\Psi_{3/2}^S \Psi_{-3/2}^J; \Psi_{-3/2}^S \Psi_{3/2}^J; \Psi_{1/2}^S \Psi_{-1/2}^J; \Psi_{-1/2}^S \Psi_{1/2}^J\}$, generating $|F, 0\rangle$ states. By calculating the exchange Hamiltonian using these wave functions as bra and ket functions, we can obtain a 4×4 matrix, the eigenvalues of which give us the same energy differences as in Eq. (6).

Thus, the main idea for microscopic calculation of A via exchange integrals is to consider the first-order correction to the energies of d -states and of the hole state due to the Coulomb interaction calculated using only these four wave functions with appropriate symmetrization and antisymmetrization of all multiparticle orbitals and spin states.

B. Microscopic calculation of exchange integrals

Wave functions of the bound Γ_8 hole corresponding to the total moment $J = 3/2$ include envelope and Bloch parts. Within the framework of the effective mass method for shallow acceptors in cubic semiconductors in the spherical approximation, the wave function of this hole is the sum of the products of the Bloch amplitudes X_μ and the smooth envelopes $R_0(r)$ and $R_2(r)$

$$\Psi_{3/2}^J = R_0(r)Y_{00}X_{3/2} + \frac{1}{\sqrt{5}}R_2(r)Y_{20}X_{3/2} \\ - \sqrt{\frac{2}{5}}R_2(r)Y_{21}X_{1/2} + \sqrt{\frac{2}{5}}R_2(r)Y_{22}X_{-1/2}, \quad (7)$$

$$\Psi_{1/2}^J = R_0(r)Y_{00}X_{1/2} - \frac{1}{\sqrt{5}}R_2(r)Y_{20}X_{1/2} \\ + \sqrt{\frac{2}{5}}R_2(r)Y_{2,-1}X_{3/2} + \sqrt{\frac{2}{5}}R_2(r)Y_{22}X_{-3/2}, \quad (8)$$

$$\Psi_{-1/2}^J = R_0(r)Y_{00}X_{-1/2} - \frac{1}{\sqrt{5}}R_2(r)Y_{20}X_{-1/2} \\ + \sqrt{\frac{2}{5}}R_2(r)Y_{2,1}X_{-3/2} + \sqrt{\frac{2}{5}}R_2(r)Y_{2,-2}X_{3/2}, \quad (9)$$

$$\Psi_{-3/2}^J = R_0(r)Y_{00}X_{-3/2} + \frac{1}{\sqrt{5}}R_2(r)Y_{20}X_{-3/2} \\ - \sqrt{\frac{2}{5}}R_2(r)Y_{2,-1}X_{-1/2} + \sqrt{\frac{2}{5}}R_2(r)Y_{2,-2}X_{1/2}, \quad (10)$$

where Y_{lm} are the spherical functions corresponding to the orbital moment l and its projection m . The exchange interaction integral will involve these functions and the d -shell wave functions, which are located in one elementary cell at the impurity site. We can neglect the effect of $R_2(r)$ functions because they tend to the zero limit at the magnetic impurity site, while $R_0(r)$ functions take nonzero values (see the calculations results in Ref. [16]). Thus, in the Appendix we calculate all exchange integrals using only Bloch parts of the Γ_8 hole wave functions, setting $\Psi_\mu^J \approx f(0)X_\mu$, where $f(0) = R_0(0)/\sqrt{4\pi}$.

Based on spin configurations of wave functions ψ_i ($i = 1, 2, 3, 4$),

$$\{\Psi_{3/2}^S \Psi_{-3/2}^J; \Psi_{-3/2}^S \Psi_{3/2}^J; \Psi_{1/2}^S \Psi_{-1/2}^J; \Psi_{-1/2}^S \Psi_{1/2}^J\}, \quad (11)$$

we can show that the Hamiltonian of the Coulomb interaction has the following 4×4 matrix form in this basis:

$$\hat{H}_C = \begin{pmatrix} \mathcal{X} & \mathcal{Z} & 0 & 0 \\ \mathcal{Z} & \mathcal{Y} & \mathcal{V} & 0 \\ 0 & \mathcal{V} & \mathcal{Y} & \mathcal{Z} \\ 0 & 0 & \mathcal{Z} & \mathcal{X} \end{pmatrix}. \quad (12)$$

The details of the calculation can be seen in the Appendix, where the true microscopical multiparticle structure of all wave functions is taken into account. Here we represent the results

$$\mathcal{X} = \langle \Psi_{3/2}^S \Psi_{-3/2}^J | U(\mathbf{r}_1 - \mathbf{r}_2) | \Psi_{3/2}^S \Psi_{-3/2}^J \rangle \\ = W + \mathfrak{x}|f(0)|^2, \quad (13)$$

$$\mathcal{Y} = \langle \Psi_{1/2}^S \Psi_{-1/2}^J | U(\mathbf{r}_1 - \mathbf{r}_2) | \Psi_{1/2}^S \Psi_{-1/2}^J \rangle \\ = W + \frac{7}{3}\mathfrak{x}|f(0)|^2, \quad (14)$$

$$\mathcal{Z} = \langle \Psi_{3/2}^S \Psi_{-3/2}^J | U(\mathbf{r}_1 - \mathbf{r}_2) | \Psi_{1/2}^S \Psi_{-1/2}^J \rangle \\ = \frac{2\sqrt{2}}{\sqrt{3}}\mathfrak{x}|f(0)|^2, \quad (15)$$

$$\mathcal{V} = \langle \Psi_{1/2}^S \Psi_{-1/2}^J | U(\mathbf{r}_1 - \mathbf{r}_2) | \Psi_{-1/2}^S \Psi_{1/2}^J \rangle \\ = 2\mathfrak{x}|f(0)|^2. \quad (16)$$

Here the Coloumb potential is used, which is given by the expression

$$U(\mathbf{r}_1 - \mathbf{r}_2) = \frac{e^2}{|\mathbf{r}_1 - \mathbf{r}_2|}. \quad (17)$$

Note that we treat the Coloumb interaction between the localized hole and holes in the d -shell (as empty states in the half-filled shell), and hence we have the positive sign in Eq. (17). The W terms in Eqs. (13) and (14) could be excluded from the consideration because they result in an equal general energy shift of all four states due to the Coloumb interaction. The main result is the connection of \mathcal{X} , \mathcal{Y} , \mathcal{Z} , and \mathcal{V} terms with the exchange integral \mathfrak{a} , which reads as

$$\mathfrak{a} = \sum_{j=1}^5 \iint_{\Omega} \frac{d\mathbf{r}_1 d\mathbf{r}_2}{15} \varphi^{j*}(\mathbf{r}_1) \varphi^j(\mathbf{r}_2) U(\mathbf{r}_1 - \mathbf{r}_2) \chi^*(\mathbf{r}_2) \chi(\mathbf{r}_1), \quad (18)$$

where the integrations go over the directly doubled GaAs-crystal elementary cell volume Ω , the sum is taken over all five one-electron orbitals of the $3d$ -shell of the manganese ion φ^j (the upper index numerates all possible orbital states $j = 1, \dots, 5$), and there is an overlapping with a p -like Bloch part of the localized hole wave function χ defined in the Appendix after Eqs. (A1) to (A4).

The eigenvalues of matrix (12) give us the following energy differences between eigenstates of this system:

$$\begin{aligned} E_2 - E_1 &= \frac{4}{3} \mathfrak{a} |f(0)|^2, & E_3 - E_2 &= 2\mathfrak{a} |f(0)|^2, \\ E_4 - E_3 &= \frac{8}{3} \mathfrak{a} |f(0)|^2. \end{aligned} \quad (19)$$

One can see from Eq. (6) that they give the same ratio between the energy differences as in the phenomenological approach using Hamiltonian (1). These results totally coincide if one puts

$$A = \frac{2}{3} \mathfrak{a} |f(0)|^2. \quad (20)$$

The later expression gives us the tool for microscopic calculations of the external forces' effects on the exchange constant A , which is relevant for many measurements.

C. Exchange constant dependence on deformation

From the symmetry point of view, the possible dependence of the exchange constant on deformation reads as

$$\hat{H} = A_0(\hat{\mathbf{S}} \cdot \hat{\mathbf{J}}) + B_P \text{Tr}(\hat{\varepsilon})(\hat{\mathbf{S}} \cdot \hat{\mathbf{J}}) + C_P \sum_{i,j} \hat{S}_i \hat{J}_j \varepsilon_{ij}. \quad (21)$$

If one considers hydrostatic deformation, the constant A depends only on the trace of the deformation tensor $\varepsilon_{ij} = \delta_{ij} \text{Tr}(\hat{\varepsilon})/3$ (here δ_{ij} is the Kronecker delta symbol)

$$\hat{H} = A_0(\hat{\mathbf{S}} \cdot \hat{\mathbf{J}}) + (B_P + C_P/3) \text{Tr}(\hat{\varepsilon})(\hat{\mathbf{S}} \cdot \hat{\mathbf{J}}). \quad (22)$$

Further, we will neglect the dependence of the envelope wave functions $f(0)$ on deformation ε because their change is too small (it is in the order of 1% of the observed values [23]).

To understand the microscopic foundations of such a Hamiltonian dependence on deformation, we assume that the true wave functions of the p -type forming the Bloch eigenstates of the valley band could be admixed by some other

atomic states, for example, via the pd hybridization mechanism keeping the total symmetry of the state unchanged. Such hybridization can occur for different reasons, for example, due to the lack of inversion symmetry in the T_d group or the action of some internal potentials. We suggest here to consider the admixing mechanism stemming from the existence of random electric fields that are commonly present near Mn impurity centers in GaAs [16].

There are several reasons for the presence of random fields in real GaMnAs crystals. The first reason is the difference in the lattice constants of a pure GaAs crystal and MnAs crystals with a zinc-blend lattice symmetry [35]; thus when the Mn ion replaces the Ga atom in the GaAs lattice an additional local stress arises, which induces a local change of lattice structure. Second, Mn ions could also be interlocated between lattice atoms, which besides another local distortion results in the formation of double manganese donor complexes. As all other donors these ones compensate for the single Mn acceptors producing local electric fields of a random direction on a site (see, for example, Ref. [36]). Finally, the Raman scattering measurements on single Mn ions demonstrate very broad lines in its spectrum compared with, however, resolvable differences between resonant energy levels, which indirectly marks the crucial role of local distortions and averaging over them [24]. The effect of random fields was treated using the perturbation approach found in Ref. [37], and it was also considered as a much greater effect than the exchange splitting of the Γ_8 hole bound on the Mn acceptor in GaAs in Ref. [28].

Such random fields are usually considered as an additional source of fine-structure splittings in the Mn acceptor energy spectrum [16,24], but they also could affect local wave functions of bound holes, i.e., the Bloch wave functions due to the pd hybridization. Thus, in Eq. (18) the χ functions should be substituted by the hybridized combinations like

$$\tilde{\chi} \approx \chi + \sum_d \gamma_d \varphi^d, \quad \tilde{\varphi}^d \approx \varphi^d - \gamma_d^* \chi, \quad \gamma_d = \frac{(\varphi^d | \hat{V} | \chi)}{E_p - E_d}. \quad (23)$$

Here E_p and E_d represent the pure atomic energies of pure p - and d -states without hybridization $E_p - E_d \sim 1$ eV (we assume here that for the Mn-acceptor in GaAs, the pure d -state lies not very far from the top of the valence band, and hence pd interaction is the largest one), and term $\hat{V} = \mathbf{r} \cdot \mathbf{F}$ stands for the hybridization operator admixing one state to another via the electro-dipole induction mechanism, which is due to some local random electric force \mathbf{F} . This force could be very sensible to the change of the elementary cell if the deformation of the crystal occurs

$$F'_i = F_i + \alpha \varepsilon_{ij} F_j. \quad (24)$$

Here we introduce dimensionless parameter α that takes into account the deformation dependence of random fields. We assume that the applied stress is a small parameter of the theory, so $\alpha \varepsilon \ll 1$, and further we take into account only the linear terms on stress.

Thus, we can estimate the change of \mathfrak{a} under a pressure or a temperature-affected widening using the following

assumptions about local electric force properties:

$$\hat{V}^2 \approx r_i r_k (F_i F_k + \alpha \varepsilon_{km} F_i F_m + \alpha \varepsilon_{ij} F_j F_k),$$

$$\langle \langle F_i \rangle \rangle = 0, \quad \langle \langle F_i F_j \rangle \rangle = \zeta \delta_{ij}.$$

Here the double angle brackets represent averaging by possible realizations of random forces. Of course, the true averaging should be processed over observable values, although the mean value of an observable depends on deformation approximately the same way as the observable calculated with such an averaged value of the exchange constant.

Finally, we can conclude that after averaging by random forces Eq. (18) could be represented by the following terms:

$$\mathfrak{a} \approx \mathfrak{a}_{ppdd} + \sum_{l,i} \mathfrak{a}_{dddd}^{ll} \frac{\langle \chi | r_i | \varphi^l \rangle \langle \varphi^l | r_i | \chi \rangle}{(E_p - E_d)^2} \zeta \left(1 + \frac{2}{3} \alpha \text{Tr}(\hat{\varepsilon}) \right), \quad (25)$$

where

$$\mathfrak{a}_{ppdd} = \sum_{j=1}^5 \iint_{\Omega} \frac{dr_1 dr_2}{15} \varphi^{j*}(\mathbf{r}_1) \varphi^j(\mathbf{r}_2) U(\mathbf{r}_1 - \mathbf{r}_2) \times \chi^*(\mathbf{r}_2) \chi(\mathbf{r}_1),$$

$$\mathfrak{a}_{dddd}^{ln} = \sum_{j=1}^5 \iint_{\Omega} \frac{dr_1 dr_2}{15} \varphi^{j*}(\mathbf{r}_1) \varphi^j(\mathbf{r}_2) U(\mathbf{r}_1 - \mathbf{r}_2) \times \varphi^{l*}(\mathbf{r}_2) \varphi^n(\mathbf{r}_1),$$

which are exchange integrals with different integrand functions. We should note that the values of these terms depend on the functions' overlap, and hence the more d -functions of Mn ion involved, the larger the value of the Coulomb term is $\mathfrak{a}_{ppdd} \ll \mathfrak{a}_{dddd}$.

To estimate the magnitude of the effect, we first take into account that all exchange integrals between d -functions have the same value in sum in Eq. (25). Then using the hydrogen atom functions χ corresponding to $4p$ orbitals and φ^d corresponding to $3d$ orbitals we can obtain an estimate $\mathfrak{a}_{dddd}/\mathfrak{a}_{ppdd} \approx 10^4$. Also, we can take the matrix elements of the coordinates approximately equal to the Bohr radius of the atom $\langle \chi | r_i | \varphi^l \rangle \approx \langle \varphi^l | r_i | \chi \rangle \approx a_B \approx 10^{-8}$ cm, and the value of the random forces' dispersion could be estimated as having the order of a typical interatomic interaction term $\sqrt{\zeta} = F_* \approx 10^6$ eV/cm (which is comparable with typical values of the mean force affecting the nuclear complex of the lattice cell in GaAs in the case of the Cu ion, for which $F \approx 5 \times 10^6$ eV/cm [38,39]). Then we can write an estimate for exchange constant A changing with deformation ($A_P \equiv B_P + C_P/3$)

$$A = A_0 + A_P \text{Tr}(\hat{\varepsilon}), \quad (26)$$

where

$$\frac{A_P}{A_0} \approx \frac{2}{3} \alpha \frac{[15(a_B F_*)^2 / (E_p - E_d)^2] \mathfrak{a}_{dddd} / \mathfrak{a}_{ppdd}}{1 + [15(a_B F_*)^2 / (E_p - E_d)^2] \mathfrak{a}_{dddd} / \mathfrak{a}_{ppdd}}. \quad (27)$$

From the data analysis found in Ref. [24], we can estimate alpha as $A_P/A_0 = (900 \text{ meV}/2.5 \text{ meV}) \approx 360$, which is equivalent to the relative change of A nearly by $\delta A/A_0 \sim \alpha \text{Tr}(\varepsilon) \sim 0.2$ at half of the critical strain of the GaAs crystal corresponding to the hardness limit at helium temperatures.

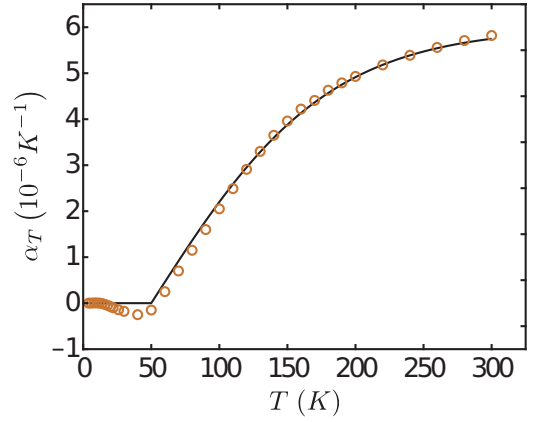


FIG. 1. Temperature dependence of linear expansion coefficient α_T . Dark orange circles are experimental results from [41] (see Table 80 on p. 233), black line is our interpolation for this dependence up to 300 K.

III. CALCULATIONS AND DISCUSSION

We discussed above the parametric dependence of exchange constant value on crystal deformation and its microscopic reasons. This fact already played its role in the explanation of Raman scattering experiment results [24], and now we are going to demonstrate clearly that the same fact is responsible for the high-temperature magnetic susceptibility reduction measured independently in a completely different experimental setting [16].

As the GaAs crystal undergoes thermal expansion, we test our hypothesis of this expansion being responsible for the anomalous reduction of magnetic susceptibility at relatively high temperatures. The temperature dependence of the linear expansion coefficient α_T could be found in the literature (see, for example, Refs. [40] or [41]). We show this dependence in Fig. 1.

We will use a simple function to interpolate the α_T dependence on temperature, which makes the interpolation work up to 300 K quite well (see Fig. 1)

$$\tilde{\alpha}_T = \begin{cases} 0, & T < 50 \text{ K}, \\ C \tanh\left(\frac{T-50}{180-50}\right), & 50 \text{ K} \leq T \leq 300 \text{ K}. \end{cases} \quad (28)$$

It is implied that T is measured in kelvins. The coefficient $C = 6 \times 10^{-6} \text{ K}^{-1}$. Note that there is a slight increase in the α_T coefficient above 300 K (at 800 K it reaches $7.4 \times 10^{-6} \text{ K}^{-1}$, see the full table of its values in Ref. [41]), and hence the approximation in Eq. (28) does not work if $T > 300$ K. For our purposes it is enough to consider the region of $T < 300$ K in which the interpolation in Eq. (28) describes the experimental data quite well. Note that a very small decrease in α_T values between 25 K and 50 K does not affect the observables in any reasonable manner, thus, we neglect it.

We are interested in the temperature range $T = 0-300$ K. So we can write the dependence of the exchange value A on T taking into account Eq. (26)

$$A(T) = A_0 + A_P \cdot 3\tilde{\alpha}_T \cdot T, \quad (29)$$

where $A_0 = 2.6 \text{ meV}$ [24]. We multiplied $\tilde{\alpha}_T$ by a factor of 3 to get the bulk thermal expansion coefficient from

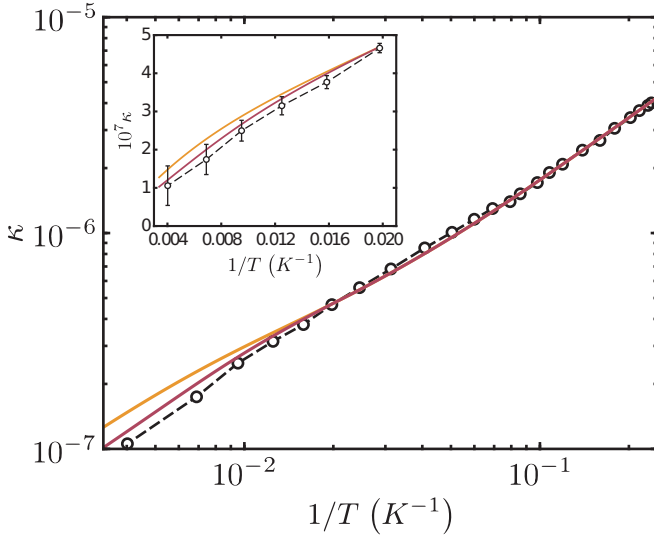


FIG. 2. Temperature dependence of static magnetic susceptibility κ of manganese ions in GaAs crystal (concentration of manganese ions $5.3 \times 10^{18} \text{ cm}^{-3}$). Both axes have logarithmic scale. Black circles connected by dashed lines represent experimental data from [16,25]. Light orange solid line is a result of calculation based on the ordinary theory from [16], which implies that $A(T) = A_0 = 2.6 \text{ meV}$. Violet solid line represents our calculation result, where the expression for magnetic susceptibility taken from [16] is modified by taking into account the exchange constant variation with temperature $A(T)$ due to the thermal expansion effect.

the linear one because $\text{Tr}(\varepsilon) = \varepsilon_{xx}(T) + \varepsilon_{yy}(T) + \varepsilon_{zz}(T) = 3\varepsilon_{xx}(T)$. Here we use the same value of $A_P = 900 \text{ meV}$ as in Ref. [24]. One can see the calculations results in Fig. 2. Note that in Ref. [16] the electron-hole basis was used, hence one should change the sign of the exchange constant into the opposite one compared with the our result to obtain the same order of energy levels for the manganese acceptor. Thus, substituting Eq. (29) into the formulas in Ref. [16], we need to multiply $A(T)$ by (-1) .

As can be seen from Fig. 2 the relative mismatch between the theory and experimental results at $T > 100 \text{ K}$ reduces approximately from 50% to 20%, if we use Eq. (29). This reduction of the systematic mismatch leads to a better agreement between theoretical results and the experimental data in the high-temperature region, which have the allowable magnitude of the experimental error (see the discussion in Ref. [16]; the experimental data were first obtained in Ref. [25], and the same mismatch was also independently mentioned in Ref. [26]). Also we point out that the sign of the changes of the exchange interaction constant, which we use to fit the magnetic susceptibility data, is the same as was used in Raman experiments [24]. Note that other possible factors, such as the crystal field effect or the reduction of magnetic susceptibility caused by the dynamical Jahn-Teller effect observed by us in Ref. [27], give no pronounced effects on magnetic susceptibility. Moreover, their effects diminish at high temperatures and they also ruin the well-established theory predictions at low temperatures below 50 K.

Thus, the effect of the exchange constant parametric dependence on lattice deformation is the only effect that provides

a reasonable explanation of both high- and low-temperature behavior characteristics of the manganese acceptor center in GaAs. Note also that $A(T)$ at $T = 300 \text{ K}$ is nearly three times larger than A_0 , and it could reach even higher values at higher temperatures according to Ref. [41] and Eq. (29). Note that at such big changes in A the nonlinear terms on lattice deformation should be also taken into account in the pd hybridization mechanism of exchange constant renormalization via random fields as soon as the parameter $\alpha \text{Tr}(\varepsilon)$ reaches and exceeds the limit of 1. We show in Fig. 2 that even linear terms give the right trend in the temperature dependence of magnetic susceptibility.

IV. CONCLUSION

The exchange constant value between d -electrons of manganese ion impurity in GaAs crystal and the hole, localized from the valence band on the impurity ion, is microscopically derived. The effect of the crystal lattice period change on the value of the exchange coupling constant occurring via the hybridization of exchanging orbitals is shown and estimated. We also discuss the effect of the thermal expansion causing the change in magnetic susceptibility. We show that accounting for this effect leads to a better agreement between theoretical results and magnetic susceptibility data measured at high temperatures. The considered thermal widening mechanism does not influence the low-temperature magnetic susceptibility behavior. This result is also in agreement with another experiment of Raman scattering on Mn acceptors in GaAs with applied external strain. We believe that the approach to the analytical calculation of the exchange constant could be generalized to the case of other magnetic centers in semiconductor structures and semi-magnetic compounds.

ACKNOWLEDGMENTS

I.V.K. and K.A.B. acknowledge the support of the Russian Science Foundation (analytical theory–Project No. 18-72-10111). K.A.B. thanks the Theoretical Physics and Mathematics Advancement Foundation “BASIS.” We also thank M. O. Nestoklon, S. A. Tarasenko, and M. M. Glazov for fruitful discussions.

APPENDIX: CALCULATION OF EXCHANGE INTEGRALS

The localized-on-the-ion hole has the Bloch part of the wave function, which describes both spin and orbital degrees of freedom in the Γ_8 -state

$$\Psi_{3/2}^J = -\alpha \frac{X + iY}{\sqrt{2}} f(0), \quad (\text{A1})$$

$$\Psi_{1/2}^J = \left(\sqrt{\frac{2}{3}} \alpha Z - \beta \frac{X + iY}{\sqrt{6}} \right) f(0), \quad (\text{A2})$$

$$\Psi_{-1/2}^J = \left(\sqrt{\frac{2}{3}} \beta Z + \alpha \frac{X - iY}{\sqrt{6}} \right) f(0), \quad (\text{A3})$$

$$\Psi_{-3/2}^J = \beta \frac{X - iY}{\sqrt{2}} f(0). \quad (\text{A4})$$

Here α and β means spin-up and spin-down states of the hole captured and localized from the valley band of the GaAs crystal, respectively. Space orbitals X , Y , and Z correspond to p -like orbitals, which form the valley band of the crystal, and hence they are quite similar to each other from the cubic symmetry point of view. So we will use more compact notations as $\chi^+ = -(X + iY)/\sqrt{2}$ and $\chi^- = (X - iY)/\sqrt{2}$.

The half-filled $3d$ -shell of the Mn ion is described by a five-hole wave function with the totally symmetrical spin part. We assume that Hund's rule is the most powerful here, and all spin-spin interactions in the shell already led to the appearance of codirected spins of all five d -holes resulting in the total spin $S = 5/2$; hence it has an antisymmetric orbital part

$$\Psi_{S_z}^S = \Phi_{1,2,3,4,5}^d |S, S_z\rangle, \quad (\text{A5})$$

$$\Phi_{1,2,3,4,5}^d = \frac{1}{\sqrt{5!}} \begin{vmatrix} \varphi_1^1 & \varphi_1^2 & \varphi_1^3 & \varphi_1^4 & \varphi_1^5 \\ \varphi_2^1 & \varphi_2^2 & \varphi_2^3 & \varphi_2^4 & \varphi_2^5 \\ \varphi_3^1 & \varphi_3^2 & \varphi_3^3 & \varphi_3^4 & \varphi_3^5 \\ \varphi_4^1 & \varphi_4^2 & \varphi_4^3 & \varphi_4^4 & \varphi_4^5 \\ \varphi_5^1 & \varphi_5^2 & \varphi_5^3 & \varphi_5^4 & \varphi_5^5 \end{vmatrix}, \quad (\text{A6})$$

$$|S, 5/2\rangle = \Theta_{1,2,3,4,5}^{5/2} = \alpha_1 \alpha_2 \alpha_3 \alpha_4 \alpha_5,$$

$$|S, 3/2\rangle = \Theta_{1,2,3,4,5}^{3/2} \quad (\text{A7})$$

$$= \frac{1}{\sqrt{5}} (\alpha_1 \alpha_2 \alpha_3 \alpha_4 \beta_5 + \alpha_1 \alpha_2 \alpha_3 \beta_4 \alpha_5 + \dots), \quad (\text{A8})$$

$$|S, 1/2\rangle = \Theta_{1,2,3,4,5}^{1/2} = \frac{1}{\sqrt{10}} (\alpha_1 \alpha_2 \alpha_3 \beta_4 \beta_5 + \alpha_1 \alpha_2 \beta_3 \alpha_4 \beta_5 + \dots + \alpha_1 \alpha_2 \beta_3 \beta_4 \alpha_5 + \dots). \quad (\text{A9})$$

The lower indices of the d -holes' orbital coordinates $\mathbf{r}_1, \mathbf{r}_2, \mathbf{r}_3, \mathbf{r}_4, \mathbf{r}_5$ are the lower indices $k = 1, 2, 3, 4, 5$ of the functions in Eq. (A6). The upper indices of the φ_k^j functions list five d -shell different orbitals $j = 1, 2, 3, 4, 5$. According to Hund's rule we take all five possible d -orbitals for the ground state of the ion because the states with identical orbital functions (and hence with opposite directions of spins) correspond to the excited states of the Mn ion having the excitation energy of electronvolts and they are out of consideration. Spin coordinates of different d -holes are also marked by the corresponding indices. The dots in the brackets of Eqs. (A8) and (A9) mean that all possible permutations of four α and one β for Eq. (A8) and three α and two β for Eq. (A9) over d -hole indices are taken into account. Wave functions corresponding to the negative projections of the total spin on the z axis $S_z = -1/2, -3/2, -5/2$ are the same if one changes all α to β and vice versa. The normalization constants for those wave functions are equal to one over the square root of the number of permutations of the α and β positions in each case, i.e., $1/\sqrt{C_5^2} = 1/\sqrt{10}$, $1/\sqrt{C_5^1} = 1/\sqrt{5}$, $1/\sqrt{C_5^0} = 1$, respectively.

Thus, we have five d -holes in the $3d$ -shell, where the strongest Coloumb interaction already led to the realization of Hund's rule, and there is the sixth localized-on-the-ion hole in the Γ_8 state, which interacts with all five d -holes. Let us introduce the potential energy operator of the remaining

weaker Coloumb interactions between the particles

$$\hat{U} = \sum_{i=1}^5 U(\mathbf{r}_i - \mathbf{r}_6). \quad (\text{A10})$$

Let us calculate the first diagonal element of such a Coloumb operator in the basis of zero total-momentum projection functions. Using the notation introduced above, we can write an antisymmetrized form of the wave function

$$\Psi_{3/2}^S \Psi_{-3/2}^J = \frac{f(0)}{\sqrt{6}} \left\{ \Phi_{1,2,3,4,5}^d \Theta_{1,2,3,4,5}^{3/2} \chi_6^- \beta_6 - \Phi_{1,2,3,4,6}^d \Theta_{1,2,3,4,6}^{3/2} \chi_5^- \beta_5 - \Phi_{1,2,3,6,5}^d \Theta_{1,2,3,6,5}^{3/2} \chi_4^- \beta_4 - \dots \right\}. \quad (\text{A11})$$

This many-particle wave function is formed by the multiplication of the wave functions of the localized hole and of five d -holes with the fixed order of their coordinates ($i = 1, 2, 3, 4, 5$), followed by the subtraction of all possible multiples with consequently interchanged coordinates of the localized hole ($i = 6$) and the d -shell holes. We can prove that this procedure gives us the antisymmetric total wave function of the system in accordance with the properties of the determinant columns' interchange.

Here we illustrate this result with the example of a three-electron system. If one has an antisymmetric combination of two electron wave functions $\phi_{1,2} = \phi_1 \psi_2 - \phi_2 \psi_1$ with the fixed order of arguments, then one can show that the procedure gives us the fully antisymmetric wave function when adding the third electron

$$\begin{aligned} & \phi_{1,2} \chi_3 - \phi_{1,3} \chi_2 - \phi_{3,2} \chi_1 \\ &= (\phi_1 \psi_2 - \phi_2 \psi_1) \chi_3 - (\phi_1 \psi_3 - \phi_3 \psi_1) \chi_2 \\ & \quad - (\phi_3 \psi_2 - \phi_2 \psi_3) \chi_1 \\ &= \begin{vmatrix} \phi_1 & \phi_2 & \phi_3 \\ \psi_1 & \psi_2 & \psi_3 \\ \chi_1 & \chi_2 & \chi_3 \end{vmatrix}. \end{aligned} \quad (\text{A12})$$

Then

$$\begin{aligned} \mathcal{X} &= \langle \Psi_{3/2}^S \Psi_{-3/2}^J | U(\mathbf{r}_1 - \mathbf{r}_2) | \Psi_{3/2}^S \Psi_{-3/2}^J \rangle \\ &= \frac{|f(0)|^2}{6} \int d\mathbf{r}_1 \dots d\mathbf{r}_6 \\ & \quad \times (\Phi_{1,2,3,4,5}^{d*} \Theta_{1,2,3,4,5}^{3/2\dagger} \chi_6^* \beta_6^\dagger - (5)^\dagger - (4)^\dagger - \dots) \\ & \quad \times \hat{U} \times (\Phi_{1,2,3,4,5}^d \Theta_{1,2,3,4,5}^{3/2} \chi_6 \beta_6 - (5) - (4) - \dots) \\ &= W + \mathfrak{x} |f(0)|^2, \end{aligned} \quad (\text{A13})$$

where the notation (5), (4), and so on are introduced for the terms in which the localized hole index 6 (and hence its coordinate \mathbf{r}_6) is swapped with the corresponding intershell d -hole indices 5, 4, and so on.

The Coloumb term W is determined by the direct product of the multiples of the same type as it is shown on the scheme

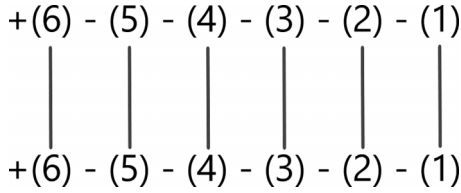


FIG. 3. The scheme of bra and ket direct multiples in Eq. (A13). The total number of direct multiples is equal to 6.

in Fig. 3 below, and it reads as

$$W = |f(0)|^2 \iint d\mathbf{r}_1 d\mathbf{r}_2 |\chi^-(\mathbf{r}_1)|^2 \sum_{j=1}^5 |\varphi^j(\mathbf{r}_2)|^2 U(\mathbf{r}_1 - \mathbf{r}_2). \quad (\text{A14})$$

The exchange term is given by Eq. (18), where χ stands for χ^- and the numerical prefactor stems from the normalization of the wave functions and the convolution of the spin wave functions with all possible cross-multiples with permutable indices, which are shown in Figs 4(a) to 4(e). Note that all multiples give the same contribution but with different signs. Thus, we carry out the calculations for the case of the multiplication of Eqs. (6) and (5) terms shown in Fig. 4(a) and take proper account of the summation of all terms with positive and negative signs

$$\Theta_{1,2,3,4,5}^{3/2\dagger} \Theta_6^\dagger \Theta_{1,2,3,4,6}^{3/2} \beta_5 [-5 \times 2 + (4 + 3 + 2 + 1) \times 2] = 2. \quad (\text{A15})$$

Note also that the remaining orbital part of the exchange integral (after the summation by the spin indices) has the following form:

$$\begin{aligned} \mathfrak{a} &= \frac{2}{6} \int d\mathbf{r}_1 \dots d\mathbf{r}_6 \chi_6^* \chi_5 \Phi_{1,2,3,4,5}^{d*} \Phi_{1,2,3,4,6}^d \\ &\quad \times [U(|\mathbf{r}_5 - \mathbf{r}_6|) + \dots] \\ &= \frac{1}{3} \times \frac{4!}{5!} \iint d\mathbf{r}_5 d\mathbf{r}_6 \chi_6^* \chi_5 \sum_{j=1}^5 \varphi_5^{j*} \varphi_6^j U(|\mathbf{r}_5 - \mathbf{r}_6|). \quad (\text{A16}) \end{aligned}$$

The integration with all terms denoted by dots in the first part of Eq. (A16) gives us zero due to the orthogonality of all orbital wave functions. The summation over the d -orbital indices in the last part of the equation is carried out considering only one index $j = 1, \dots, 5$ for both one-particle functions φ_5^{j*} and φ_6^j . The latter could be easily checked by treating the multiples in explicit forms written one under another as

$$\chi_6^* \Phi_{1,2,3,4,5}^{d*} = \frac{\chi_6^*}{\sqrt{5!}} (\varphi_1^1 \varphi_2^2 \varphi_3^3 \varphi_4^4 \varphi_5^5 - \varphi_1^1 \varphi_2^2 \varphi_3^3 \varphi_5^4 \varphi_4^5 + \dots)^*, \quad (\text{A17})$$

$$\chi_5 \Phi_{1,2,3,4,6}^d = \frac{\chi_5}{\sqrt{5!}} (\varphi_1^1 \varphi_2^2 \varphi_3^3 \varphi_4^4 \varphi_6^5 - \varphi_1^1 \varphi_2^2 \varphi_3^3 \varphi_6^4 \varphi_4^5 + \dots). \quad (\text{A18})$$

Here the first term is determined by the fixed sequence of the coordinate indices and all others are determined by the coordinate indices' swapping accompanied by a change of the sign. One can see that the nonzero multiples are only those which are the products of two terms written strictly under each other in Eqs. (A17) and (A18). All other multiples give us

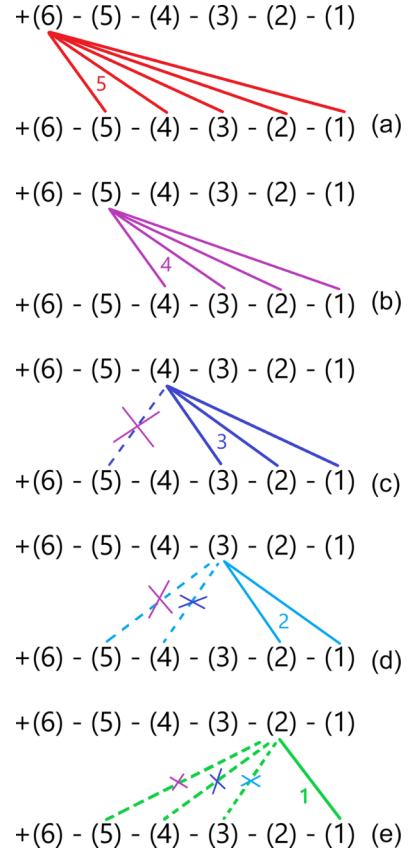


FIG. 4. The scheme of bra and ket cross-multiples in Eq. (A13). (a) There are $5 \times 2 = 10$ cross-multiples with the minus sign if one considers five cross-multiples in the inset and their mirror twins emerging as if the virtual reflection in the horizontal plane takes place. (b)–(e) The number of each multiple of the plus sign should be multiplied by 2 due to the same reason as discussed for inset (a). The total number of multiples equals to $(4 + 3 + 2 + 1) \times 2 = 20$.

zero due to the mutual orthogonality of all functions. Thus, all terms are summed up only with positive signs. The number of such summands with fixed position of fifth and sixth particles equal to the number of permutations of the other four electrons over the remaining four orbitals and hence it is equal to $4! = 24$.

Let us explain now, in brief, the calculation details for the \mathcal{Y} , \mathcal{Z} , and \mathcal{V} terms. The \mathcal{Y} term also involves bra and ket functions of the same type

$$\begin{aligned} \Psi_{1/2}^S \Psi_{-1/2}^J &= \frac{f(0)}{\sqrt{6}} \left\{ \Phi_{1,2,3,4,5}^d \Theta_{1,2,3,4,5}^{1/2} \left(\sqrt{\frac{2}{3}} Z_6 \beta_6 + \sqrt{\frac{1}{3}} \chi_6^- \alpha_6 \right) \right. \\ &\quad \left. - (5) - (4) - \dots \right\}. \quad (\text{A19}) \end{aligned}$$

Here the same notation [(5), (4), etc.] is introduced as for Eq. (A13). One can see that the same scheme which we used when calculating the matrix elements of the direct Coulomb interaction terms gives us, as denoted in Fig. 3, the same value W (due to the symmetry properties of χ^- and Z functions of the localized hole), and the latter could be excluded from consideration. The exchange terms' calculation requires consideration of two possible results of the wave function's spin

parts' convolution. The first is

$$\begin{aligned} & \Theta_{1,2,3,4,5}^{1/2\dagger} \beta_6^\dagger \Theta_{1,2,3,4,6}^{1/2} \beta_5 \\ &= \frac{1}{10} (\alpha_1^\dagger \alpha_2^\dagger \alpha_3^\dagger \beta_4^\dagger \beta_5^\dagger + \alpha_1^\dagger \alpha_2^\dagger \beta_3^\dagger \alpha_4^\dagger \beta_5^\dagger + \dots) \beta_6^\dagger \\ & \quad \times (\alpha_1 \alpha_2 \alpha_3 \beta_4 \beta_6 + \alpha_1 \alpha_2 \beta_3 \alpha_4 \beta_6 + \dots) \beta_5 \\ &= \frac{1}{10} (\alpha_1^\dagger \alpha_2^\dagger \alpha_3^\dagger \beta_4^\dagger + \alpha_1^\dagger \alpha_2^\dagger \beta_3^\dagger \alpha_4^\dagger + \dots) \\ & \quad \times (\alpha_1 \alpha_2 \alpha_3 \beta_4 + \alpha_1 \alpha_2 \beta_3 \alpha_4 + \dots) = \frac{4}{10}, \quad (\text{A20}) \end{aligned}$$

and the second is

$$\begin{aligned} & \Theta_{1,2,3,4,5}^{1/2\dagger} \alpha_6^\dagger \Theta_{1,2,3,4,6}^{1/2} \alpha_5 \\ &= \frac{1}{10} (\alpha_1^\dagger \alpha_2^\dagger \alpha_3^\dagger \beta_4^\dagger \beta_5^\dagger + \alpha_1^\dagger \alpha_2^\dagger \beta_3^\dagger \alpha_4^\dagger \beta_5^\dagger + \dots) \alpha_6^\dagger \\ & \quad \times (\alpha_1 \alpha_2 \alpha_3 \beta_4 \beta_6 + \alpha_1 \alpha_2 \beta_3 \alpha_4 \beta_6 + \dots) \alpha_5 \\ &= \frac{1}{10} (\alpha_1^\dagger \alpha_2^\dagger \beta_3^\dagger \beta_4^\dagger + \alpha_1^\dagger \beta_2^\dagger \alpha_3^\dagger \beta_4^\dagger + \dots) \\ & \quad \times (\alpha_1 \alpha_2 \beta_3 \beta_4 + \alpha_1 \beta_2 \alpha_3 \beta_4 + \dots) = \frac{6}{10}. \quad (\text{A21}) \end{aligned}$$

Then, after the summation over the spin indices and taking into account possible cross-multiples, as in Figs. 4(a) to 4(e), we obtain an additional multiplier $[-5 \times 2 + (4+3+2+1) \times 2] = 10$ as in Eq. (A15), and then we get the exchange part of \mathcal{V} equal to

$$\begin{aligned} & |f(0)|^2 \frac{10}{6} \int d\mathbf{r}_1 \dots d\mathbf{r}_6 \left(\frac{2}{3} \frac{4}{10} Z_6^* Z_5 + \frac{1}{3} \frac{6}{10} \chi_6^* \chi_5 \right) \\ & \quad \times \Phi_{1,2,3,4,5}^{d*} \Phi_{1,2,3,4,6}^d (U(|\mathbf{r}_5 - \mathbf{r}_6|) + \dots) \\ &= |f(0)|^2 \frac{7}{9} \times \frac{4!}{5!} \iint d\mathbf{r}_5 d\mathbf{r}_6 \chi_6^* \chi_5 \\ & \quad \times \sum_{j=1}^5 \varphi_5^{j*} \varphi_6^j U(|\mathbf{r}_5 - \mathbf{r}_6|) = \frac{7}{3} \mathfrak{a} |f(0)|^2. \quad (\text{A22}) \end{aligned}$$

Here we use the symmetry equivalence of Z and χ functions when calculating such types of integrals.

When calculating \mathcal{Z} , the off-diagonal matrix element between quantum states from Eq. (A11) and Eq. (A19) is taken. Thus, there is no Coloumb term and the exchange integral in this case reads as

$$\begin{aligned} \mathcal{Z} &= |f(0)|^2 \frac{10}{6} \int d\mathbf{r}_1 \dots d\mathbf{r}_6 \Phi_{1,2,3,4,5}^{d*} \Theta_{1,2,3,4,5}^{3/2\dagger} \chi_6^{-*} \beta_6^\dagger \\ & \quad \times \hat{U} \Phi_{1,2,3,4,6}^d \Theta_{1,2,3,4,6}^{1/2} \left(\sqrt{\frac{2}{3}} Z_5 \beta_5 + \sqrt{\frac{1}{3}} \chi_5^- \alpha_5 \right) \\ &= |f(0)|^2 \frac{10}{6} \int d\mathbf{r}_1 \dots d\mathbf{r}_6 \Phi_{1,2,3,4,5}^{d*} \Theta_{1,2,3,4,5}^{3/2\dagger} \chi_6^{-*} \beta_6^\dagger \\ & \quad \times \hat{U} \Phi_{1,2,3,4,6}^d \Theta_{1,2,3,4,6}^{1/2} \sqrt{\frac{1}{3}} \chi_5^- \alpha_5. \quad (\text{A23}) \end{aligned}$$

The multiplier 10 arises as a result of the usage of the introduced scheme, which implies taking into account all exchange integrals [see Figs. 4(a) to 4(e)]. There are no multiples with Z functions because the convolution of the spin functions gives zero, as the considered summands have 4α and 1β parts of

$\Theta_{1,2,3,4,5}^{3/2\dagger}$ spin function, and 3α and 2β enter $\Theta_{1,2,3,4,6}^{1/2}$ spin function. The spin convolution of the latter part is equal to

$$\begin{aligned} & \Theta_{1,2,3,4,5}^{3/2\dagger} \beta_6^\dagger \Theta_{1,2,3,4,6}^{1/2} \alpha_5 \\ &= \frac{1}{\sqrt{5}} (\alpha_1^\dagger \alpha_2^\dagger \alpha_3^\dagger \alpha_4^\dagger \beta_5^\dagger + \alpha_1^\dagger \alpha_2^\dagger \alpha_3^\dagger \beta_4^\dagger \alpha_5^\dagger + \dots) \beta_6^\dagger \\ & \quad \times \frac{1}{\sqrt{10}} (\alpha_1 \alpha_2 \alpha_3 \beta_4 \beta_6 + \alpha_1 \alpha_2 \beta_3 \alpha_4 \beta_6 + \dots) \alpha_5 \\ &= \frac{1}{\sqrt{50}} (\alpha_1^\dagger \alpha_2^\dagger \alpha_3^\dagger \beta_4^\dagger + \alpha_1^\dagger \alpha_2^\dagger \beta_3^\dagger \alpha_4^\dagger + \dots) \\ & \quad \times (\alpha_1 \alpha_2 \alpha_3 \beta_4 + \alpha_1 \alpha_2 \beta_3 \alpha_4 + \dots) = \frac{4}{\sqrt{50}}. \quad (\text{A24}) \end{aligned}$$

Then finally we get

$$\begin{aligned} \mathcal{Z} &= |f(0)|^2 \frac{10}{6} \frac{4}{\sqrt{50}} \frac{1}{\sqrt{3}} \frac{4!}{5!} \iint d\mathbf{r}_5 d\mathbf{r}_6 \chi_6^* \chi_5 \\ & \quad \times \sum_{j=1}^5 \varphi_5^{j*} \varphi_6^j U(|\mathbf{r}_5 - \mathbf{r}_6|) = \frac{2\sqrt{2}}{\sqrt{3}} \mathfrak{a} |f(0)|^2. \quad (\text{A25}) \end{aligned}$$

The calculation of another off-diagonal matrix element \mathcal{V} requires usage of the following ket wave function according to Eq. (16):

$$\begin{aligned} & \Psi_{-1/2}^S \Psi_{1/2}^J \\ &= \frac{f(0)}{\sqrt{6}} \left\{ \Phi_{1,2,3,4,5}^d \Theta_{1,2,3,4,5}^{-1/2} \left(\sqrt{\frac{2}{3}} Z_6 \alpha_6 + \sqrt{\frac{1}{3}} \chi_6^+ \beta_6 \right) \right. \\ & \quad \left. - (5) - (4) - \dots \right\}. \quad (\text{A26}) \end{aligned}$$

As the spin function $\Theta_{1,2,3,4,5}^{1/2}$ contains 3α and 2β in each summation term, while the function $\Theta_{1,2,3,4,5}^{-1/2}$, on the contrary, contains 2α and 3β in each summand, one can see that the exchange matrix element of the interaction between quantum states given by Eqs. (A19) and Eq. (A26) will reduce to the following expression, having nonzero contributions from only Z -orbital terms:

$$\begin{aligned} \mathcal{V} &= |f(0)|^2 \frac{10}{6} \int d\mathbf{r}_1 \dots d\mathbf{r}_6 \Phi_{1,2,3,4,5}^{d*} \Theta_{1,2,3,4,5}^{1/2\dagger} \\ & \quad \times \sqrt{\frac{2}{3}} Z_6^* \beta_6^\dagger \hat{U} \Phi_{1,2,3,4,6}^d \Theta_{1,2,3,4,6}^{-1/2} \sqrt{\frac{2}{3}} Z_5 \alpha_5 \\ &= |f(0)|^2 \frac{10}{6} \frac{2}{3} \frac{6}{10} \frac{4!}{5!} \iint d\mathbf{r}_5 d\mathbf{r}_6 Z_6^* Z_5 \\ & \quad \times \sum_{j=1}^5 \varphi_5^{j*} \varphi_6^j U(|\mathbf{r}_5 - \mathbf{r}_6|) = 2\mathfrak{a} |f(0)|^2, \quad (\text{A27}) \end{aligned}$$

in which the result of the spin function's convolution is included

$$\begin{aligned} & \Theta_{1,2,3,4,5}^{1/2\dagger} \beta_6^\dagger \Theta_{1,2,3,4,6}^{-1/2} \beta_5 \\ &= \frac{1}{10} (\alpha_1^\dagger \alpha_2^\dagger \alpha_3^\dagger \beta_4^\dagger \beta_5^\dagger + \alpha_1^\dagger \alpha_2^\dagger \beta_3^\dagger \alpha_4^\dagger \beta_5^\dagger + \dots) \beta_6^\dagger \\ & \quad \times (\beta_1 \beta_2 \beta_3 \alpha_4 \alpha_6 + \beta_1 \beta_2 \alpha_3 \beta_4 \alpha_6 + \dots) \alpha_5 \\ &= \frac{1}{10} (\alpha_1^\dagger \alpha_2^\dagger \beta_3^\dagger \beta_4^\dagger + \dots) (\alpha_1 \alpha_2 \beta_3 \beta_4 + \dots) = \frac{6}{10}. \quad (\text{A28}) \end{aligned}$$

- [1] D. D. Awschalom and M. E. Flatté, *Nat. Phys.* **3**, 153 (2007).
- [2] B. R. Ortiz, L. C. Gomes, J. R. Morey, M. Winiarski, M. Bordelon, J. S. Mangum, I. W. H. Oswald, J. A. Rodriguez-Rivera, J. R. Neilson, S. D. Wilson, E. Ertekin, T. M. McQueen, and E. S. Toberer, *Phys. Rev. Mater.* **3**, 094407 (2019).
- [3] M. M. Otrokov, I. P. Rusinov, M. Blanco-Rey, M. Hoffmann, A. Yu. Vyazovskaya, S. V. Eremeev, A. Ernst, P. M. Echenique, A. Arnau, and E. V. Chulkov, *Phys. Rev. Lett.* **122**, 107202 (2019).
- [4] M. Gibertini, M. Koperski, A. F. Morpurgo, and K. S. Novoselov, *Nat. Nanotechnol.* **14**, 408 (2019).
- [5] M.-C. Wang, C.-C. Huang, C.-H. Cheung, C.-Y. Chen, S. G. Tan, T.-W. Huang, Y. Zhao, Y. Zhao, G. Wu, Y.-P. Feng *et al.*, *Ann. Phys. (Leipzig)* **532**, 1900452 (2020).
- [6] D. Jena, R. Page, J. Casamento, P. Dang, J. Singhal, Z. Zhang, J. Wright, G. Khalsa, Y. Cho, and H. G. Xing, *Jpn. J. Appl. Phys.* **58**, SC0801 (2019).
- [7] E. Y. Tsymbal and I. Žutić, *Spintronics Handbook: Spin Transport and Magnetism*, 2nd ed. (CRC Press, Boca Raton, FL, 2019).
- [8] Q. D. Gibson, L. M. Schoop, L. Muechler, L. S. Xie, M. Hirschberger, N. P. Ong, R. Car, and R. J. Cava, *Phys. Rev. B* **91**, 205128 (2015).
- [9] K. F. Mak and J. Shan, *Nat. Nanotechnol.* **17**, 686 (2022).
- [10] R. F. Need, S.-K. Bac, X. Liu, S. Lee, B. J. Kirby, M. Dobrowolska, J. Kossut, and J. K. Furdyna, *Phys. Rev. Mater.* **4**, 054410 (2020).
- [11] J. Furdyna, J. Leiner, X. Liu, M. Dobrowolska, S. Lee, J. Chung, and B. Kirby, *Acta Phys. Pol. A* **121**, 973 (2012).
- [12] M. Mogi, Y. Okamura, M. Kawamura, R. Yoshimi, K. Yasuda, A. Tsukazaki, K. Takahashi, T. Morimoto, N. Nagaosa, M. Kawasaki *et al.*, *Nat. Phys.* **18**, 390 (2022).
- [13] A. McCreary, J. R. Simpson, T. T. Mai, R. D. McMichael, J. E. Douglas, N. Butch, C. Dennis, R. Valdés Aguilar, and A. R. High Walker, *Phys. Rev. B* **101**, 064416 (2020).
- [14] K. F. Mak, J. Shan, and D. C. Ralph, *Nat. Rev. Phys.* **1**, 646 (2019).
- [15] I. Krainov, V. Sapega, G. Dimitriev, and N. Averkiev, *J. Phys.: Condens. Matter* **33**, 445802 (2021).
- [16] N. Averkiev and A. Gutkin, *Phys. Solid State* **60**, 2311 (2018).
- [17] S. Lee, J.-H. Chung, X. Liu, J. K. Furdyna, and B. J. Kirby, *Mater. Today* **12**, 14 (2009).
- [18] T. Jungwirth, J. Sinova, J. Mašek, J. Kučera, and A. H. MacDonald, *Rev. Mod. Phys.* **78**, 809 (2006).
- [19] Y. Yuan, C. Xu, R. Hübner, R. Jakiela, R. Böttger, M. Helm, M. Sawicki, T. Dietl, and S. Zhou, *Phys. Rev. Mater.* **1**, 054401 (2017).
- [20] X. Liu and J. K. Furdyna, *J. Phys.: Condens. Matter* **18**, R245 (2006).
- [21] A. Yakunin, A. Y. Silov, P. Koenraad, J.-M. Tang, M. Flatté, J.-L. Primus, W. Van Roy, J. De Boeck, A. Monakhov, K. Romanov *et al.*, *Nat. Mater.* **6**, 512 (2007).
- [22] A. Monakhov, N. Sablina, N. Averkiev, C. Çelebi, and P. Koenraad, *Solid State Commun.* **146**, 416 (2008).
- [23] M. Nestoklon, O. Krebs, R. Benchamekh, and P. Voisin, *Semicond. Sci. Technol.* **30**, 035019 (2015).
- [24] I. V. Krainov, J. Debus, N. S. Averkiev, G. S. Dimitriev, V. F. Sapega, and E. Lähderanta, *Phys. Rev. B* **93**, 235202 (2016).
- [25] D. G. Andrianov, Y. N. Bol'sheva, G. V. Lazareva, A. S. Savel'ev, and S. M. Yakubeny, *Fiz. Tekh. Poluprovodn.* **17**, 810 (1983) [*Sov. Phys. Semicond.* **17**, 506 (1983)].
- [26] T. Frey, M. Maier, J. Schneider, and M. Gehrke, *J. Phys. C* **21**, 5539 (1988).
- [27] See Supplemental Material at <http://link.aps.org/supplemental/10.1103/PhysRevB.107.174401> for the effects of the crystal field (part 1) and the Jahn-Teller effect (part 2).
- [28] I. Y. Karlik, I. Merkulov, D. Mirlin, L. Nikitin, V. Perel, and V. Sapega, *Fiz. Tverd. Tela* **24**, 3550 (1982) [*Sov. Phys. Solid State* **24**, 2022 (1982)].
- [29] N. S. Averkiev, A. A. Gutkin, N. M. Kolchanova, and M. A. Reschikov, *Fiz. Tekh. Poluprovodn.* **18**, 1629 (1984) [*Sov. Phys. Semicond.* **18**, 1019 (1984)].
- [30] N. S. Averkiev, A. A. Gutkin, E. B. Osipov, and M. A. Reschikov, *Fiz. Tekh. Poluprovodn.* **21**, 1847 (1987) [*Sov. Phys. Semicond.* **21**, 1119 (1987)].
- [31] J. Schneider, U. Kaufmann, W. Wilkening, M. Baumler, and F. Köhl, *Phys. Rev. Lett.* **59**, 240 (1987).
- [32] I. B. Bersuker, *The Jahn-Teller Effect*, 1st ed. (Cambridge University Press, Cambridge England, 2006).
- [33] V. Sapega, T. Ruf, and M. Cardona, *Phys. Status Solidi (b)* **226**, 339 (2001).
- [34] K. I. Kugel and D. Khomskii, *Sov. Phys. Usp.* **25**, 231 (1982).
- [35] V. F. Sapega, M. Moreno, M. Ramsteiner, L. Däweritz, and K. Ploog, *Phys. Rev. B* **66**, 075217 (2002).
- [36] T. Jungwirth, K. Y. Wang, J. Mašek, K. W. Edmonds, J. König, J. Sinova, M. Polini, N. A. Goncharuk, A. H. MacDonald, M. Sawicki, A. W. Rushforth, R. P. Campion, L. X. Zhao, C. T. Foxon, and B. L. Gallagher, *Phys. Rev. B* **72**, 165204 (2005).
- [37] N. S. Averkiev, A. A. Gutkin, E. Osipov, and M. Reschikov, *Fiz. Tverd. Tela* **30**, 765 (1988) [*Sov. Phys. Solid State* **30**, 438 (1988)].
- [38] K. Baryshnikov, N. Averkiev, A. Monakhov, and V. Gudkov, *Phys. Solid State* **54**, 468 (2012).
- [39] N. Averkiev, I. Bersuker, V. Gudkov, K. Baryshnikov, I. Zhevstovskikh, V. Y. Mayakin, A. Monakhov, M. Sarychev, V. Sedov, and V. Surikov, *J. Appl. Phys.* **116**, 103708 (2014).
- [40] New semiconductor materials. Biology systems. Characteristics and properties, <http://www.ioffe.ru/SVA/NSM/Semicond/GaAs/thermal.html>.
- [41] S. I. Novikova, *Thermal Expansion of Solids (Russian book)* (Izdatel'stvo Nauka, Moscow, 1974).